

Published in final edited form as:

*Magn Reson Imaging*. 2011 April ; 29(3): 324–334. doi:10.1016/j.mri.2010.09.004.

## Quantitative MRI using $T_{1\rho}$ and $T_2$ in human osteoarthritic cartilage specimens: Correlation with biochemical measurements and histology

Xiaojuan Li, PhD<sup>1</sup>, Jonathan Cheng, MS<sup>1</sup>, Katrina Lin, BS<sup>1</sup>, Ehsan Saadat, BS<sup>1</sup>, Radu I. Bolbos, PhD<sup>1</sup>, Michael D. Ries, MD<sup>2</sup>, Andrew Horvai, MD<sup>3</sup>, Thomas M. Link, MD<sup>1</sup>, and Sharmila Majumdar, PhD<sup>1</sup>

Jonathan Cheng: chengbermusik@gmail.com; Katrina Lin: katrinajlin@gmail.com; Ehsan Saadat: Ehsan.Saadat@ucsf.edu; Radu I. Bolbos: radu.bolbos@gmail.com; Michael D. Ries: riesm@orthosurg.ucsf.edu; Andrew Horvai: andrew.horvai@ucsf.edu; Thomas M. Link: Thomas.Link@radiology.ucsf.edu; Sharmila Majumdar: sharmila.majumdar@radiology.ucsf.edu

<sup>1</sup>Musculoskeletal and Quantitative Imaging Research, Department of Radiology and Biomedical Imaging, University of California, San Francisco (UCSF), CA

<sup>2</sup>Department of Orthopaedic Surgery, UCSF, San Francisco, CA

<sup>3</sup>Department of Pathology, UCSF, San Francisco, CA

### Abstract

**Purpose**—A direct correlation between  $T_{1\rho}$ ,  $T_2$  and quantified proteoglycan and collagen contents in human osteoarthritic cartilage has yet to be documented. We aimed to investigate the orientation effect on  $T_{1\rho}$  and  $T_2$  values in human osteoarthritic cartilage; and to quantify the correlation between  $T_{1\rho}$ ,  $T_2$ , versus biochemical composition and histology in human osteoarthritic cartilage.

**Materials and Methods**—Thirty-three cartilage specimens were collected from patients who underwent total knee arthroplasty due to severe osteoarthritis, and scanned with a 3T MR scanner for  $T_{1\rho}$  and  $T_2$  quantification. Nine specimens were scanned at three different orientations with respect to the  $B_0$ :  $0^\circ$ ,  $90^\circ$ , and  $54.7^\circ$ . Core punches were taken after MRI. Collagen and proteoglycan contents were quantified using biochemical assays. Histology sections were graded using Mankin scores. The correlation between imaging parameters, biochemical contents and histological scores were studied.

**Results**—Both mean  $T_{1\rho}$  and  $T_2$  at  $54.7^\circ$  were significantly higher than those measured at  $90^\circ$  and  $0^\circ$ , with  $T_{1\rho}$  showing a less increase compared to  $T_2$ .  $R_{1\rho}$  ( $1/T_{1\rho}$ ) values had a significant, but moderate correlation with proteoglycan contents ( $R = 0.45$ ,  $P = 0.002$ ), while  $R_2$  ( $1/T_2$ ) was not correlated with proteoglycan. No significant correlation was found between relaxation times ( $T_{1\rho}$  or  $T_2$ ) and collagen contents. The  $T_{1\rho}$  values of specimen sections with high Mankin scores were significantly higher than those with low Mankin scores ( $P < 0.05$ )

© 2010 Elsevier Inc. All rights reserved.

Corresponding author: Xiaojuan Li, PhD, Department of Radiology and Biomedical Imaging, University of California, San Francisco, 185 Berry Street, Suite 350, San Francisco, CA 94107, xiaojuan.li@radiology.ucsf.edu, Tel: 415-353-4909; Fax: 415-353-9425.

**Publisher's Disclaimer:** This is a PDF file of an unedited manuscript that has been accepted for publication. As a service to our customers we are providing this early version of the manuscript. The manuscript will undergo copyediting, typesetting, and review of the resulting proof before it is published in its final citable form. Please note that during the production process errors may be discovered which could affect the content, and all legal disclaimers that apply to the journal pertain.

### Competing Interest

The authors declare that they have no competing interests.

**Conclusions**—Quantitative MRI has a great potential to provide non-invasive imaging biomarkers for cartilage degeneration in OA.

### Keywords

Osteoarthritis; Magnetic Resonance Imaging; Cartilage matrix; T1rho; T2

## INTRODUCTION

Osteoarthritis affects over 20 million people in the US alone and is highly prevalent in the aging population [1]. It is a heterogeneous and multifactorial disease characterized primarily by the progressive loss of hyaline articular cartilage [2]. Hyaline cartilage consists of a relatively small number of chondrocytes embedded in an extracellular matrix formed mainly of collagen fibers, proteoglycans (PGs) and water. Three distinct structural zones are defined based on the orientation of the collagen fibers: the superficial zone at the surface characterized by collagen fibrils that are oriented parallel to the articular surface, the transitional zone characterized by randomly oriented collagen fibers, and the radial (deep) zone characterized by a perpendicular arrangement of collagen fibrils to the subchondral bone [3].

The current clinical evaluation of cartilage degeneration in OA relies primarily on plain radiography, which depicts only gross osseous changes that occur late in the disease. While standard clinical magnetic resonance imaging (MRI) techniques afford better clinical accuracy, these techniques are still limited to providing primarily morphological changes of cartilage, which are only secondary effects of the damage to the collagen-PG matrix of cartilage. Quantitative MRI techniques, including  $T_{1\rho}$  and  $T_2$  relaxation time quantification [4–8] and delayed gadolinium-enhanced MRI in cartilage (dGEMRIC) [9], have been developed to study changes in biochemical concentration and structure of macromolecules [10–12]. In particular,  $T_{1\rho}$  and  $T_2$  quantification techniques require no contrast agent injection and have great promising to be used widely in clinical settings. The ability to assess changes of the collagen-PG matrix using non-invasive MRI may provide early biomarkers of the onset of osteoarthritis and would allow early intervention of cartilage degeneration at the earliest stages.

In order to elucidate the specificity and mechanism of  $T_{1\rho}$  and  $T_2$  in cartilage imaging, several studies have quantified  $T_{1\rho}$  and  $T_2$  in protein solutions and cartilage specimens [7,13–15]. Using enzymatic degradation of bovine cartilage, Akella et al established that  $T_{1\rho}$  is sensitive for PG content while  $T_2$  is not [7]. Furthermore, Regatte and colleagues found  $T_{1\rho}$  and  $T_2$  to increase with OA clinical grade in human total knee arthroplasty specimens [14]. However, a direct correlation between  $T_{1\rho}$ ,  $T_2$  and quantified PG and collagen contents in fresh human OA cartilage has yet to be documented.

We questioned whether there was an orientation effect in reference to the external magnetic  $B_0$  on  $T_{1\rho}$  and  $T_2$  quantification, as this orientation effect may serve as an impeding factor between a direct correlation of  $T_{1\rho}$  and  $T_2$  relaxation times and biochemical composition of cartilage. The orientation effect of  $T_2$  has been well documented in cartilage specimens [16–18] and *in vivo* [19]. However, very few studies have investigated such effect in  $T_{1\rho}$  [20].

The goals of this study were therefore twofold: 1) to investigate the orientation effect on  $T_{1\rho}$  and  $T_2$  values in human osteoarthritic articular cartilage; and 2) to systematically quantitatively evaluate the correlation between  $T_{1\rho}$ ,  $T_2$ , versus biochemical composition (PG and collagen) and histology in human osteoarthritic cartilage specimens.

## MATERIALS AND METHODS

### Specimen collection

Human specimens containing cartilage and bone were collected from sixteen knees of fifteen patients (one patient had a bilateral knee operation). All the patients underwent total knee arthroplasty (TKA) due to severe OA by an experienced orthopaedic surgeon (MDR) at the UCSF arthritis and joint replacement center. Patients with prior knee surgery, inflammatory arthritis, or post traumatic arthritis were excluded. The study protocol was approved by the Human Research Committee of our institute. Before specimen collection, written informed consent was obtained from all patients after the nature of the examinations had been fully explained.

During TKA, five specimens were resected in a standardized fashion by the orthopedic surgeon (MDR): tibia plateau (containing medial tibia [MT] and lateral tibia [LT]), medial/lateral inferior femoral condyle (MIFC and LIFC), medial/lateral posterior femoral condyle (MPFC and LPFC), as shown in Figure 1. We studied specimens obtained from the side with less advanced degeneration and therefore enough residual cartilage for imaging and biochemical analysis.

After resection, the specimens were labeled with blue ink mark at the anterior end of tibia plateau, LIFC and MIFC, and inferior end of LPFC and MPFC for future orientation references. The specimens were then wrapped in Ringer's Lactate-soaked gauze, transported and stored at 4°C for less than 48 hours before *ex vivo* specimen MRI. No freezing was performed before and during the whole procedure of this study to avoid any potential effect of freezing on cartilage matrix biochemistry. The specimens were stored at -80°C after the study.

### *Ex vivo* MR Imaging

The cartilage specimens were scanned within 48 hours after surgery on a GE 3T Signa MRI scanner (GE Healthcare, Milwaukee, WI, USA) using a quadrature transmit/receive wrist coil (Mayo Foundation for Medical Education and Research, Rochester, MN, USA). Before the MR scan, the knee cartilage specimens were mounted on a plastic grid for location reference as shown in Figure 2. Simethicone was applied to cartilage surface to minimize biochemical exchanges between specimens and solution, and to help reduce accumulation of small air bubbles on tissue surface. The specimens were then placed and glued into a plastic container and immersed in phosphate-buffered saline (PBS). A thin plastic tube serving as a marker was placed on top of the specimen and defined the location of histological sectioning performed after MRI (Figure 2). After preparation, the specimens were stored at room temperature for approximately thirty minutes before the MR scan.

Among the specimens studied, nine were scanned at three different orientations with respect to the  $B_0$ : 0°, 90°, and 54.7°, Figure 3. The 54.7° is correlated with the geometrical factor ( $3\cos^2\theta - 1$ ) that governs the dipolar Hamiltonian. The angles were assessed relative to the radial zone, to maintain consistency with previous studies [16,18,20]. All other specimens were scanned in their respective physiological positions to simulate their *in vivo* orientation and position. Consequently the tibial (LT and MT) and inferior femoral condyle (LIFC and MIFC) pieces were scanned in a horizontal position while the posterior femoral condyle (LPFC and MPFC) specimens were scanned in a vertical position within the scanner, aligning the radial zone at 90° and 0° with respect to  $B_0$ .

The imaging protocol included sagittal T<sub>2</sub>-weighted fat-saturated fast spin-echo (FSE) images (TR/TE = 4300/51 ms, FOV = 6–8 cm, matrix = 512×256, slice thickness = 1 mm, echo train length = 9, bandwidth = 31.25 kHz, NEX = 2) and sagittal 3D fat suppressed

high-resolution spoiled gradient-echo (SPGR) images (TR/TE = 15/6.7 ms, flip angle = 12, FOV = 6–8 cm, matrix = 512 × 512, slice thickness = 1 mm, bandwidth = 31.25 kHz, NEX = 1).

A sagittal 3D  $T_{1\rho}$ -weighted imaging sequence developed previously in our lab was applied in this study (MAPSS, [21]). The sequence is composed of two parts: magnetization preparation based on spin-lock techniques for the imparting of  $T_{1\rho}$  contrast, and an elliptical-centered segmented 3D SPGR acquisition immediately after  $T_{1\rho}$  preparation during transient signal evolution. The duration of the spin-lock pulse was defined as time of spin-lock (TSL), and the strength of the spin-lock pulse was defined as spin-lock frequency ( $F_{SL}$ ). There was a relatively long delay (time of recovery,  $T_{rec}$ ) between each magnetization preparation to allow enough and equal recovery of the magnetization before each  $T_{1\rho}$  preparation. The imaging parameters are: TR/TE = 9.3/3.7 ms; FOV = 6–8 cm, matrix = 256 × 128, slice thickness = 2 mm, BW = 31.25 kHz, Views Per Segment = 64,  $T_{rec}$  = 1.5 s, TSL = 0, 10, 40, 80 ms,  $F_{SL}$  = 500 Hz.

Tissue relaxation during the continuous spin-lock pulse is a complex process that depends on  $B_1$ ,  $B_0$ , and the component of parallel (relax with  $R_{1\rho}$  or  $1/T_{1\rho}$ ) and perpendicular (relax with  $R_{2\rho}$  or  $1/T_{2\rho}$ ) magnetization [22]. In spin-lock experiments for  $T_{1\rho}$  contrast, with presence of  $B_1$  and  $B_0$  heterogeneity, off axial rotation will occur, magnetization in plane perpendicular to SL pulses will relax with  $R_{2\rho}$ , and significant artifact will be observed [23]. In our experiment, we used a  $B_1$  insensitive SL pulses with a rotary echo, as proposed by Charagundla et al. [24]. Combined with a high spin-lock amplitude of 500 Hz ( $\omega_1 \gg \Delta \omega_0$ ), the regions of cartilage in our images were free from the artifacts caused by potential  $B_1$  and  $B_0$  heterogeneity. In our experiment, we titrated TG as detailed in [24] to calibrate the hard pulse to be 90°. Therefore the  $T_{2\rho}$  component with our current experimental set up would be minimal, and the magnetization relaxation will be dominated by  $T_{1\rho}$  during spin-lock.

Sagittal 3D  $T_2$  mapping were performed immediately after the  $T_{1\rho}$  quantification sequence by adding a nonselective  $T_2$  preparation refocusing pulses to the same SPGR sequence as for  $T_{1\rho}$  mapping [25]. All prescription parameters of the  $T_2$  sequence were the same as the  $T_{1\rho}$  sequence except for TR/TE = 2000/4.1, 14.5, 25, 45.9 ms..

## Biochemistry

After the imaging procedure, core samples of the cartilage with approximately 50 mg weight were obtained with a 3mm biopsy punch (Sklar Instruments, West Chester, PA). As mentioned above only the compartments with less severe degeneration, mostly in the lateral compartments of the joint, were studied to ensure there was enough residual cartilage to investigate correlation between imaging parameters, biochemistry and histology. Full thickness cartilage punches were taken with an effort to avoid underlying subchondral bone. Locations of the punches were recorded carefully using anatomical measurements from the lateral/medial and anterior/posterior edges of the specimens as well as anatomical and pathological landmarks.

The cores were digested with a papain digestion buffer at 60°C for 24 hours. Subsequently, a dimethylene blue (DMB) assay (Blyscan assay, Biocolor, UK) was performed to determine GAG content based on the manufactures' instructions. The total GAG weight was determined based on absorbance at 656 nm on a spectrophotometer. The GAG mass percentage was obtained by dividing the calculated GAG weight by the wet weight of cartilage. Aliquots were also hydrolyzed overnight with 6N HCl at 110°C prior to performing a colorimetric assay to evaluate the hydroxyproline content for collagen estimation [26,27]. Total collagen was calculated as ten times the hydroxyproline content, considering hydroxyproline comprises 10% of the weight of each collagen alpha chain [28].

## Histology

Following *ex vivo* imaging and core punching, 3mm thick sagittal histological sections in the same plane as the sagittal *ex vivo* MRI were obtained adjacent to the cores. In addition, the exact location of the histology sections was recorded carefully using anatomical and landmark measurements. These sections were fixed in 10% formalin and embedded in paraffin. Maximum length for each embedded piece was 2 cm. Therefore, the LT/MT or LIFC/MIFC were normally cut into two pieces: anterior versus posterior. The LPFC was generally maintained as one piece due to their small dimension. The samples were stained with hematoxylin and eosin (H&E) for morphological measurements and safranin-O for GAG content. Histological evaluation of articular cartilage degeneration was performed by a pathologist (AH) using the Mankin score, which describes cartilage structure, cells, safranin-O staining, and tidemark integrity (Table 1).[29]

## Ex vivo Image Processing

After scanning, all MR images were transferred to a Sun Workstation (Sun Microsystems, Palo Alto, CA) for offline post processing.

The  $T_{1\rho}$  and  $T_2$  maps were reconstructed using an in-house developed software written in C by fitting the  $T_{1\rho}$ -weighted and  $T_2$ -weighted images pixel-by-pixel to the equation  $\alpha S(TSL) S * \exp(-TSL/T_{1\rho})$  and  $S(TE) \alpha S * \exp(-TE/T_2)$ , respectively.

Cartilage was segmented semiautomatically in sagittal SPGR images using an in-house developed program with MATLAB based on edge detection and Bezier splines [30]. The locations of the punches were identified in SPGR images based on anatomical distances and landmarks, and confirmed with reference location from the plastic grid (Figure 4). The images were reviewed by at least two imaging researchers involved in this study to ensure the accurate location of the punches were identified in MR images. Three-dimensional ROIs of the full thickness of cartilage at the punch location were generated and overlaid to reconstructed  $T_{1\rho}$  and  $T_2$  maps. The mean, median and standard deviation (SD) of  $T_{1\rho}$  and  $T_2$  values from the regions corresponding to biochemical punches were calculated.

The histology sections were also cross-referenced in SPGR images based on anatomical distances and anatomical/pathological landmarks (such as osteophytes). The location was further confirmed by the reference location of the plastic tubes (Figure 5). The shape of the specimen within identified image slice was matched with the histology staining slice. The ROIs of segmented cartilage with the histology slice were overlaid on  $T_{1\rho}$  and  $T_2$  maps. For specimens of LT/MT and LIFC/MIFC, the ROIs were cut into two as anterior and posterior ROIs with equal distance, in order to correspond the histology staining. The mean, median and SD of  $T_{1\rho}$  and  $T_2$  values of these regions, i.e., the whole histological section for LPFC/MPFC, anterior and posterior histology sections for LT/MT and LIFC/MIFC, were calculated.

## Statistical analysis

One-way analysis of variation (ANOVA) was used to examine if  $T_{1\rho}$  and  $T_2$  values at different orientations differ to each other. If ANOVA indicated a significant difference, a paired t-test was used to compare  $T_{1\rho}$  and  $T_2$  values between each two different orientations.  $T_{1\rho}$  values at different spin-lock frequencies were also compared using paired t-test. Spearman correlation coefficients were calculated between relaxation times rate ( $1/T_{1\rho}$  and  $1/T_2$ ) and biochemical measurements (PG and collagen contents) using R (<http://www.r-project.org/>). Relaxation time and biochemical measurements in different regions (LIFC vs LPFC for example) were compared using t-tests.

## RESULTS

A total of 33 specimens were scanned with MRI and processed with biochemical and histological analyses. These specimens included 10 LT, 1 MT, 10 LIFC, 8 LPFC, 3 MPFC and 1 MIFC.

### **T<sub>1ρ</sub> dispersion and orientation effect on T<sub>1ρ</sub> and T<sub>2</sub> quantification**

Of the nine specimens scanned at three orientation, both mean T<sub>1ρ</sub> and T<sub>2</sub> at 54.7° were significantly higher than those measured at 90° and 0°, Table 2. The difference in T<sub>1ρ</sub> at spin-lock frequency of 500Hz between measurement at 0° and 54.7° were lower than that in T<sub>2</sub> values (10.9% in T<sub>1ρ</sub> vs 19.4% in T<sub>2</sub>). This difference was further reduced to 7.0% for T<sub>1ρ</sub> at spin-lock frequency of 1KHz. The results were similar for the difference in T<sub>1ρ</sub> and T<sub>2</sub> values between measurement at 90° and 54.7°. The mean T<sub>1ρ</sub> values increased significantly from spin-lock frequency of 500 Hz to 1K Hz at all angles (P < 0.05), showing significant T<sub>1ρ</sub> dispersion. The increase percentage was 17.2%, 20.2% and 13.0% for 90°, 0° and 54.7°, respectively.

### **Correlation between relaxation times and biochemical measurements**

In total, 46 biochemistry cores were taken from the 33 specimens: 15 from LIFC, 1 from MIFC, 9 from LPFC, 4 from MPFC, 16 from LT and 1 from MT. The mean T<sub>1ρ</sub> values of the samples were 65.8 ± 12.3 ms, ranging from 43.6 ms to 91.9 ms. The mean T<sub>2</sub> values of the samples were 39.5 ± 11.8 ms, ranging from 17.7 ms to 72.8 ms. The median R<sub>1ρ</sub> relaxation rate (1/T<sub>1ρ</sub>) corresponding to each core showed a significant, but moderate positive correlation with GAG contents (R = 0.45, P = 0.002, Figure 6). No significant correlation was found between the median R<sub>2</sub> relaxation rate (1/T<sub>2</sub>) and GAG contents (R = 0.24, P = 0.17). No significant correlation was found between relaxation time rates (1/T<sub>1ρ</sub> or 1/T<sub>2</sub>) and collagen contents (P > 0.05).

The specimens were scanned in their respective physiological positions that were the same as the *in vivo* orientation. Correlation coefficients were further calculated in subgroups of specimens that were scanned with the same orientation: Group I (n = 33): the tibial (LT and MT) and inferior femoral condyle (LIFC and MIFC) with the radial zone of cartilage at 0° with respect to the B<sub>0</sub>; and Group II (n = 13): the posterior femoral condyle pieces (LPFC and MPFC), with the radial zone of cartilage at 90° with respect to the B<sub>0</sub>. In group I, R<sub>1ρ</sub> values were correlated negatively with GAG contents (R = 0.34, P = 0.01), while R<sub>2</sub> values were not (R = 0.1, P = 0.6). No significant correlation was found between relaxation time and collagen content (P > 0.05). In group II, no significant correlation was found between relaxation times and biochemical measurements (P > 0.05), probably due to the small sample size.

### **Regional variation of biochemistry and relaxation time**

We investigated the distribution of biochemistry and relaxation times in different anatomical regions in the knee. Specifically we focused on the lateral side: LIFC, LPFC and LT, because there were not enough samples from the medial compartments in this study. The LIFC regions showed significantly higher mean GAG contents than the LPFC regions (4.5% ± 1.8% vs. 3.3% ± 0.7%, P = 0.036) (Table 3). Correspondingly, the T<sub>1ρ</sub> values of LIFC were significantly lower than those of LPFC (62.4 ± 11.8 ms vs. 76.8 ± 7.9 ms, P = 0.002). A similar difference was observed with T<sub>2</sub> relaxation time (34.3 ± 8.6 ms in LIFC vs 52.8 ± 6.7 ms in LPFC, P = 0.0002). LIFC had a lower collagen content compared to LPFC, but the difference was not significant (4.4% ± 1.8% in LIFC vs 6.9% ± 3.4% in LPFC, P = 0.095). No significant difference in biochemistry and relaxation times was observed between tibial and femoral condyle regions.

## Relationship between relaxation times and histology

No significant correlation was found between MR relaxation times and histological Mankin scores in all specimens. Among the 22 LT/MT and LIFC/MIFC specimens, 18 (6 LT, 10 LIFC, 1 MT and 1 MIFC) showed different Mankin scores between anterior and posterior portion, suggesting spatial heterogeneity of cartilage degeneration within the joint. We regrouped these specimens into two groups: group I with low Mankin scores ( $2.8 \pm 1.5$ ) vs. group II with high Mankin scores ( $5.6 \pm 1.9$ ). The  $T_{1\rho}$  values of group II with high Mankin scores were significantly higher than group I with low Mankin scores ( $70.5 \pm 14.4$  ms vs.  $64.6 \pm 12.1$  ms,  $P = 0.027$ ).  $T_2$  were slightly higher in group II than group I, but the difference was not significant ( $37.7 \pm 8.2$  ms vs.  $36.6 \pm 8.8$  ms,  $P = 0.639$ ). Figure 7 shows a representative histology slides and  $T_{1\rho}$  maps from a lateral tibial plateau specimen.

## DISCUSSION

MR  $T_{1\rho}$  and  $T_2$  relaxation quantification have been proposed as promising diagnostic tools for early detection of cartilage degeneration in OA. This study has documented the quantitative relationship between these imaging biomarkers and biochemical and histological analysis in fresh human osteoarthritic cartilage. The present work was performed in a setup resembling clinical imaging and this enables potential extension of the findings into the clinical realm.

In a subset of the specimens collected in this study, the effect of static magnetic field orientation on both  $T_{1\rho}$  and  $T_2$  relaxation times has been investigated. Although such an orientation effect in  $T_2$  relaxation time, due to the strong dipole-dipole interaction, has been well documented in cartilage [16–19], very limited studies have investigated this in  $T_{1\rho}$  [20]. In this study, we observed significantly higher  $T_2$  values at the magic angle,  $54.7^\circ$  compared to values measured at the other two positions ( $0^\circ$  and  $90^\circ$ ), which is consistent with what observed in the literature. A similar orientation effect was observed for  $T_{1\rho}$  relaxation time, but to a lesser extent compared to  $T_2$  relaxation time. The difference in  $T_{1\rho}$  values between  $0^\circ$  and  $54.7^\circ$  measured at spin-lock frequency of 500Hz were approximately half of the difference in  $T_2$  values between these two positions (10.9% in  $T_{1\rho}$  vs 19.4% in  $T_2$ ). This difference was further reduced to 7.0% for  $T_{1\rho}$  measured with spin-lock frequency of 1KHz.

The main interactions responsible for  $T_{1\rho}$  relaxation time include scalar-coupling, dipole-dipole interactions and chemical exchange processes [31]. Our results suggest that the spin-lock technique used in  $T_{1\rho}$  imaging sequence helps to reduce the dipolar interaction of the motion-restricted water protons within cartilage matrix, therefore reduce the angular dependence of  $T_{1\rho}$  on collagen fibers. The higher the spin-lock frequency, the smaller orientation effect on the  $T_{1\rho}$  relaxation time quantification. Previous studies suggested that during spin-lock proton exchange between the protein side-chain groups of GAG and bulk water may contribute significantly to the  $T_{1\rho}$  relaxation in articular cartilage [32,33].

Akella et al. observed that the orientation effect on  $T_{1\rho}$  values disappeared when the spin-lock frequency was approaching 2KHz using bovine cartilage plugs on a 4.7 Tesla small-bore MRI scanner [20]. In this study, we could not acquire the  $T_{1\rho}$ -weighted images at the high spin-lock frequency of 2KHz due to hardware limitations on the clinical whole body scanner. However, the trend was consistent with the findings reported by Akella et al [20]. This  $T_{1\rho}$  dispersion may be due to a combination of residual dipolar interaction and other processes such as chemical exchange.

In this study, a significant while moderate negative correlation between  $T_{1\rho}$  relaxation time and GAG contents measured with biochemical assays were observed. The similar trend of increasing  $T_2$  relaxation times with decreased GAG was also observed, however, the

correlation was not significant. These results in human OA cartilage were consistent with previous reports on correlating relaxation times with trypsin-induced GAG loss in bovine cartilage models [34], where a strong correlation between  $T_{1\rho}$  and GAG loss percentage ( $R^2 = 0.85$ ,  $P < 0.0001$ ) was found, while the correlation between  $T_2$  and GAG loss was poor ( $R^2 = 0.008$ ,  $P < 0.7$ ). These results suggested  $T_{1\rho}$  is more sensitive to detect PG changes in cartilage matrix than  $T_2$ .

Compared to the strong correlation observed in the bovine study, the correlation between  $T_{1\rho}$  and GAG contents in human OA samples in this study is rather moderate ( $R = -0.45$ ). As the human specimens were collected from OA patients and present a much more heterogeneous group compared to experimentally controlled samples, this lower correlation is not surprising. This moderate correlation may imply that factors in addition to GAG contents may also contribute to  $T_{1\rho}$  relaxation time changes, such as hydration and different stages of collagen degradation. No correlation was found between MR relaxation times and collagen measurements in this study. This may be partially explained by the fact that measurement of collagen content using biochemical assays is limited in providing the total amount of collagen. It cannot distinguish between different stages of collagen breakdown, which may affect MR relaxation times differently.

We have further investigated the regional variation in GAG and collagen contents. GAG contents were found to be significantly higher in the lateral inferior femoral condyle than the lateral posterior femoral condyle. This finding that the GAG contents were higher in a weight-bearing region (inferior femoral condyle) than a non-weight bearing region (posterior femoral condyle) was consistent with previous literature [35]. Specifically, previous studies have shown that GAG content increases with load [36,37]. In this study, this phenomenon was observed in a spatially specific pattern, which is also consistent with previous findings showing topographical variation in knee cartilage GAG contents [37]. Meanwhile, The  $T_{1\rho}$  values in lateral inferior femoral condyle was significantly lower than those in lateral posterior femoral condyle, showing a consistent negative correlation between  $T_{1\rho}$  values and GAG contents. No significant difference in overall collagen content was observed between sub-compartments in this study.

Histology has been used as a 'gold-standard' to evaluate cartilage degeneration in OA. Investigators have made efforts to correlation MRI with histological findings. Regatte et al. have quantified  $T_2$  and  $T_{1\rho}$  relaxation times in various clinical grades of eight human OA cartilage specimens [14]. The OA was graded by visual evaluation of the joint surface by an orthopedic surgeon and was further confirmed in representative cartilage specimens by histology. These investigators observed a significant increase of  $T_{1\rho}$  values from early OA to severe OA, with an elevation of 38.5% in early OA, 84% in moderate OA and 110.8% in severe OA compared to controls.  $T_2$  was also elevated in specimens with different grades of OA, but the magnitude of increase was very small (5–50%) compared to  $T_{1\rho}$ , and it was difficult to differentiate moderate OA from advanced OA.

In the present study, we attempted to extend the investigation on the capability of MR relaxation times to characterize disease stages by directly correlating  $T_{1\rho}$  and  $T_2$  values with histology using semi-quantitative Mankin scores. The mean Mankin score was 4.2, ranging from 1 to 9, representing from early to rather moderate OA for the specimens in this study. No significant correlation was found between  $T_{1\rho}$  or  $T_2$  values and Mankin scores in overall specimens. This lack of correlation suggested that it is challenging to apply histology for quantitative studies, especially when the staining as well as Mankin score reading are not performed in one time, which was the case for this study and would introduce potential bias/errors during the semi-quantifications.



In order to minimize any potential errors introduced by these factors, we further examined the specimens that were cut into two pieces during histology, primarily composed with lateral/medial inferior femoral condyle and lateral/medial tibial pieces. Among 22 specimens, 18 showed different Mankin scores between the anterior and posterior portions. This result suggests spatial heterogeneity of cartilage degeneration within the joint. However, there is no specific spatial distribution pattern (anterior vs posterior) with regard to low vs. high Mankin scores. Using a paired t-test, in these 18 pieces, the  $T_{1\rho}$  values in specimens with low Mankin scores were significantly lower than those with high Mankin scores, Figure 7.  $T_2$  showed a slight increase in the specimens with high Mankin scores compared to those with low Mankin scores, but the difference was not significant. These results demonstrate that there is a good correlation between  $T_{1\rho}$  relaxation time and disease severity as quantified by histological Mankin scores. The lack of such correlation between  $T_2$  and histology is consistent with findings in the literature [14], suggesting that  $T_2$  elevation in OA is not specific to disease severity.

There are a few limitations of the present study. First, in this study, we were focusing on the specimens of the less degenerated compartments, and punches for biochemical analysis normally were taken from relatively 'healthy looking' cartilage. Thus the specimens included in this study present a relatively moderate OA group (maximum Mankin score of 9) instead of a full spectrum of OA. Secondly, full thickness measurement of  $T_{1\rho}$  and  $T_2$  were used in this study. Since hyaline cartilage shows distinct characteristics of collagen and PG composition, separate analysis in different layers may increase correlation between imaging parameters and biochemical measures, and will be explored in future experiments. Third, the collagen analysis used in this study was limited to overall collagen contents, which may partially contribute to the lack of correlation between MR relaxation times and collagen contents. More advanced biochemical analysis techniques that provide information on collagen cross-link and therefore information on different stages of collagen degradation during OA may help to elucidate the correlation between MR relaxation times and changes in collagen structures.

## CONCLUSION

The major contribution of this study is the documentation the quantitative correlation between MR  $T_{1\rho}$  and  $T_2$  relaxation times and biochemical and histological measurements in fresh human OA cartilage specimens.  $T_{1\rho}$  has shown to be a good indicator for both overall cartilage health as described by the Mankin score, and GAG contents using biochemical assays.  $T_{1\rho}$ , especially with high spin-lock frequencies, showed a less orientation dependence compared to  $T_2$ . Our ultimate goal was to correlate *in vivo* non-invasive quantitative MRI with biochemical and histological analysis of degenerative cartilage, and our experimental model using *in vitro* analysis of surgical specimens came very close to this goal though limitations were encountered. Based on these results we believe that *in vivo* MR relaxation time quantification techniques have a great potential to provide non-invasive imaging biomarkers for cartilage degeneration in OA.

## Acknowledgments

The work was done at the University of California, San Francisco (UCSF). The research was supported by NIH R01 AR46905 and K25 AR053633.

## List of abbreviations

**MRI** magnetic resonance imaging

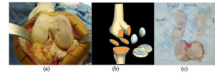
<b>OA</b>	osteoarthritis
<b>PBS</b>	phosphate-buffered saline
<b>TKA</b>	total knee arthroplasty
<b>PG</b>	proteoglycan
<b>GAG</b>	glycosaminoglycan
<b>MT</b>	medial tibia
<b>LT</b>	lateral tibia
<b>M/LIFC</b>	medial/lateral inferior femoral condyle
<b>M/LPFC</b>	medial/lateral posterior femoral condyle
<b>FSE</b>	fast spin-echo
<b>SPGR</b>	spoiled gradient-echo
<b>TSL</b>	time of spin-lock
<b>F<sub>SL</sub></b>	spin-lock frequency

## REFERENCES

1. Brandt, KD.; Doherty, M.; Lohmander, L.S., editors. Osteoarthritis. New York: Oxford University Press Inc; 1998.
2. Martin JA, Buckwalter JA. Roles of articular cartilage aging and chondrocyte senescence in the pathogenesis of osteoarthritis. *Iowa Orthop J* 2001;21:1–7. [PubMed: 11813939]
3. Verstraete KL, Almqvist F, Verdonk P, Vanderschueren G, Huysse W, Verdonk R, Verbrugge G. Magnetic resonance imaging of cartilage and cartilage repair. *Clin Radiol* 2004;59:674–689. [PubMed: 15262541]
4. Mosher TJ, Dardzinski BJ, Smith MB. Human articular cartilage: influence of aging and early symptomatic degeneration on the spatial variation of T2--preliminary findings at 3 T. *Radiology* 2000;214:259–266. [PubMed: 10644134]
5. Dunn TC, Lu Y, Jin H, Ries MD, Majumdar S. T2 relaxation time of cartilage at MR imaging: comparison with severity of knee osteoarthritis. *Radiology* 2004;232:592–598. [PubMed: 15215540]
6. Duvvuri U, Kudchodkar S, Reddy R, Leigh JS. T(1rho) relaxation can assess longitudinal proteoglycan loss from articular cartilage in vitro. *Osteoarthritis Cartilage* 2002;10:838–844. [PubMed: 12435327]
7. Akella SV, Regatte RR, Gougoutas AJ, Borthakur A, Shapiro EM, Kneeland JB, Leigh JS, Reddy R. Proteoglycan-induced changes in T1rho-relaxation of articular cartilage at 4T. *Magn Reson Med* 2001;46:419–423. [PubMed: 11550230]
8. Li X, Ma C, Link T, Castillo D, Blumenkrantz G, Lozano J, Carballido-Gamio J, Ries M, Majumdar S. In vivo T1rho and T2 mapping of articular cartilage in osteoarthritis of the knee using 3 Tesla MRI. *Osteoarthritis and Cartilage* 2007;15:789–797. [PubMed: 17307365]
9. Bashir A, Gray ML, Hartke J, Burstein D. Nondestructive imaging of human cartilage glycosaminoglycan concentration by MRI. *Magn Reson Med* 1999;41:857–865. [PubMed: 10332865]
10. Link T, Stahl R, Woertler K. Cartilage imaging: motivation, techniques, current and future significance. *Eur Radiol* 2007;17:1135–1146. [PubMed: 17093967]
11. Gold G, Chen C, Koo S, Hargreaves B, Bangerter N. Recent advances in MRI of articular cartilage. *AJR Am J Roentgenol* 2009;193:628–638. [PubMed: 19696274]
12. Burstein D, Gray M, Mosher T, Dardzinski B. Measures of molecular composition and structure in osteoarthritis. *Radiol Clin North Am* 2009;47:675–686. [PubMed: 19631075]

13. Wheaton AJ, Dodge GR, Elliott DM, Nicoll SB, Reddy R. Quantification of cartilage biomechanical and biochemical properties via T1rho magnetic resonance imaging. *Magn Reson Med* 2005;54:1087–1093. [PubMed: 16200568]
14. Regatte R, Akella S, Lonner J, Kneeland J, Reddy R. T1rho relaxation mapping in human osteoarthritis (OA) cartilage: comparison of T1rho with T2. *J Magn Reson Imaging* 2006;23:547–553. [PubMed: 16523468]
15. Menezes NM, Gray ML, Hartke JR, Burstein D. T2 and T1rho MRI in articular cartilage systems. *Magn Reson Med* 2004;51:503–509. [PubMed: 15004791]
16. Rubenstein J, Kim J, Morova-Protzner I, Stanchev P, Henkelman R. Effects of collagen orientation on MR imaging characteristics of bovine articular cartilage. *Radiology* 1993;188:219–226. [PubMed: 8511302]
17. Xia Y, Farquhar T, Burton-Wurster N, Lust G. Origin of cartilage laminae in MRI. *J Magn Reson Imaging* 1997;7:887–894. [PubMed: 9307916]
18. Xia Y. Relaxation anisotropy in cartilage by NMR microscopy (muMRI) at 14-microm resolution. *Magn Reson Med* 1998;39:941–949. [PubMed: 9621918]
19. Mosher TJ, Smith H, Dardzinski BJ, Schmithorst VJ, Smith MB. MR imaging and T2 mapping of femoral cartilage: in vivo determination of the magic angle effect. *AJR Am J Roentgenol* 2001;177:665–669. [PubMed: 11517068]
20. Akella SV, Regatte RR, Wheaton AJ, Borthakur A, Reddy R. Reduction of residual dipolar interaction in cartilage by spin-lock technique. *Magn Reson Med* 2004;52:1103–1109. [PubMed: 15508163]
21. Li X, Han E, Busse R, Majumdar S. In vivo T1rho mapping in cartilage using 3D magnetization-prepared angle-modulated partitioned k-space spoiled gradient echo snapshots (3D MAPSS). *Magn Reson Med* 2007;59:298–307. [PubMed: 18228578]
22. Sorce D, Michaeli S, Garwood M. The time-dependence of exchange-induced relaxation during modulated radio frequency pulses. *J Magn Reson* 2006;179:136–139. [PubMed: 16298149]
23. Witschey, Wn; Borthakur, A.; Elliott, M.; Mellon, E.; Niyogi, S.; Wallman, D.; Wang, C.; Reddy, R. Artifacts in T1 rho-weighted imaging: compensation for B(1) and B(0) field imperfections. *J Magn Reson* 2007;186:75–85. [PubMed: 17291799]
24. Charagundla SR, Borthakur A, Leigh JS, Reddy R. Artifacts in T(1rho)-weighted imaging: correction with a self-compensating spin-locking pulse. *J Magn Reson* 2003;162:113–121. [PubMed: 12762988]
25. Pai A, Li X, Majumdar S. A comparative study at 3 T of sequence dependence of T2 quantitation in the knee. *Magn Reson Imaging* 2008;26:1215–1220. [PubMed: 18502073]
26. Burleigh MC, Barrett AJ, Lazarus GS. Cathepsin B1. A lysosomal enzyme that degrades native collagen. *Biochem J* 1974;137:387–398. [PubMed: 4207388]
27. Hollander AP, Heathfield TF, Webber C, Iwata Y, Bourne R, Rorabeck C, Poole AR. Increased damage to type II collagen in osteoarthritic articular cartilage detected by a new immunoassay. *J Clin Inv* 1994;93:1722–1732.
28. Nimni ME. Collagen: structure, function and metabolism in normal and fibrotic tissues. *Sem Arthr Rheum* 1983;13:1–86.
29. Mankin HJ, Dorfman H, Lippiello L, Zarins A. Biochemical and metabolic abnormalities in articular cartilage from osteo-arthritic human hips. II. Correlation of morphology with biochemical and metabolic data. *J Bone Joint Surg Am* 1971;53:523–537. [PubMed: 5580011]
30. Carballido-Gamio J, Bauer JS, R S, Lee KY, Krause S, Link TM, Majumdar S. Inter-subject comparison of MRI knee cartilage thickness. *Medical Image Analysis* 2007;12:120–135. [PubMed: 17923429]
31. Borthakur A, Mellon E, Niyogi S, Witschey W, Kneeland J, Reddy R. Sodium and T1rho MRI for molecular and diagnostic imaging of articular cartilage. *NMR Biomed* 2006;19:781–821. [PubMed: 17075961]
32. Makela HI, Grohn OH, Kettunen MI, Kauppinen RA. Proton exchange as a relaxation mechanism for T1 in the rotating frame in native and immobilized protein solutions. *Biochem Biophys Res Commun* 2001;289:813–818. [PubMed: 11735118]

33. Duvvuri U, Goldberg AD, Kranz JK, Hoang L, Reddy R, Wehrli FW, Wand AJ, Englander SW, Leigh JS. Water magnetic relaxation dispersion in biological systems: the contribution of proton exchange and implications for the noninvasive detection of cartilage degradation. *Proc Natl Acad Sci U S A* 2001;98:12479–12484. [PubMed: 11606754]
34. Regatte RR, Akella SV, Borthakur A, Kneeland JB, Reddy R. Proteoglycan depletion-induced changes in transverse relaxation maps of cartilage: comparison of T2 and T1rho. *Acad Radiol* 2002;9:1388–1394. [PubMed: 12553350]
35. Urban JP. The chondrocyte: a cell under pressure. *Br J Rheumatol* 1994;33:901–908. [PubMed: 7921748]
36. Saadat E, Lan H, Majumdar S, Rempel DM, King KB. Long-term cyclical in vivo loading increases cartilage proteoglycan content in a spatially specific manner: an infrared microspectroscopic imaging and polarized light microscopy study. *Arthritis Res Ther* 2006;8:R147. [PubMed: 16956418]
37. Rogers BA, Murphy CL, Cannon SR, Briggs TW. Topographical variation in glycosaminoglycan content in human articular cartilage. *J Bone Joint Surg Br* 2006;88:1670–1674. [PubMed: 17159186]

**Figure 1.**

Cartilage specimen collection from patients with severe osteoarthritis who underwent total knee arthroplasty. (a) The open knee of a patient during TKA showing severe cartilage degeneration especially in medial side of the knee; (b) diagram of five specimens containing cartilage and bone sectioned during normal TKA: lateral/medial inferior femoral condyle (LIFC and MIFC), lateral/medial posterior femoral condyle (LPFC and MPFC), tibial plateau (containing lateral and medial tibia, LT and MT); (c) Five pieces of specimens from the patient in (a). Blue ink marked the anterior end of tibial plateau and LIFC/MIFC, and inferior end of LPFC and MPFC.

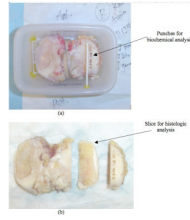


**Figure 2.**

Specimen preparation. The specimen was mounted on a plastic grid for location reference, and then placed and glued into a plastic container and immersed in phosphate-buffered saline (PBS) for ex vivo MRI (a). An additional thin plastic tube marker was placed on top of the location where the histology slice was obtained after the MRI. After MRI, punches were taken for biochemical analysis (a) and a 3mm histology slice was cut next to the biochemical punches for histological analysis (b).

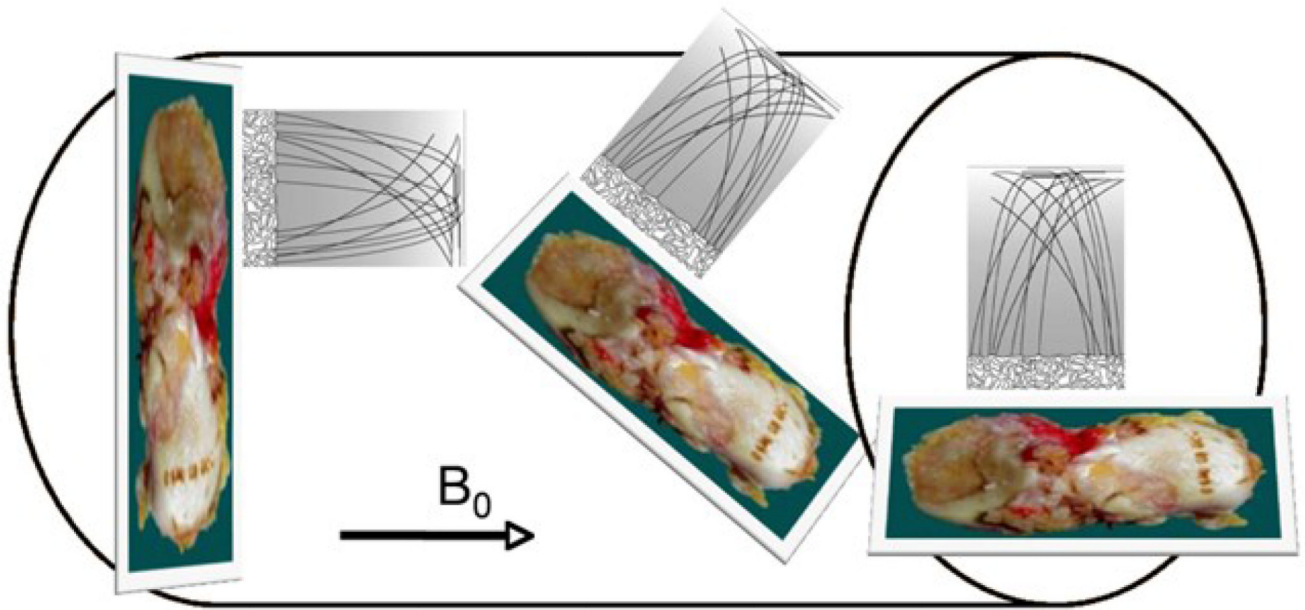


**Figure 3.** Diagram of cartilage specimens ex vivo MRI with different orientations in the MR scanner. Specimens were scanned at three different orientations with respect to the  $B_0$ : 0° (left), 54.7° (center) and 90° (right).

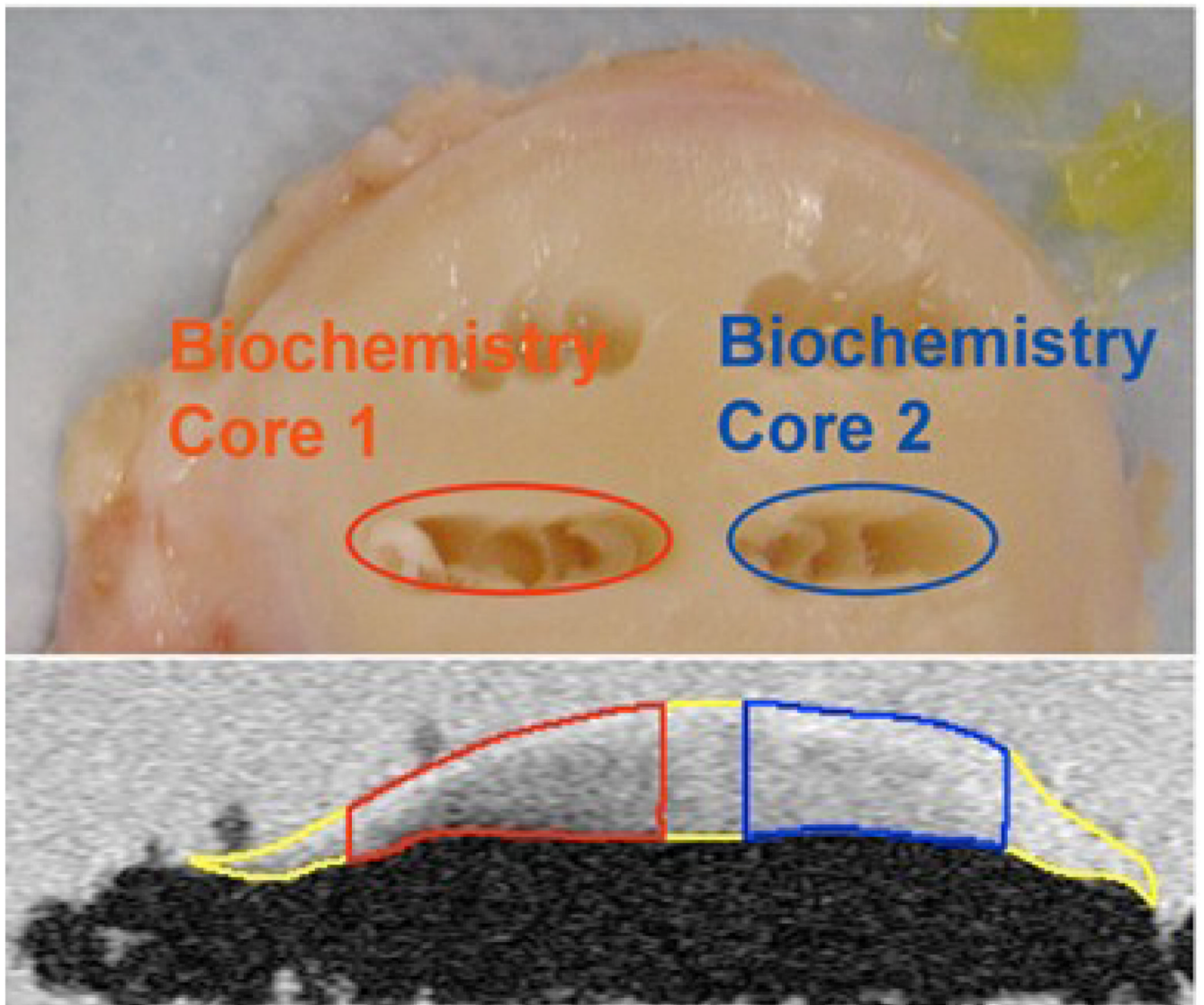


**Figure 4.** The locations of the punches for biochemical analysis (top) were identified in SPGR images (bottom) based on anatomical distances and landmarks, and confirmed with reference location from the plastic grid.



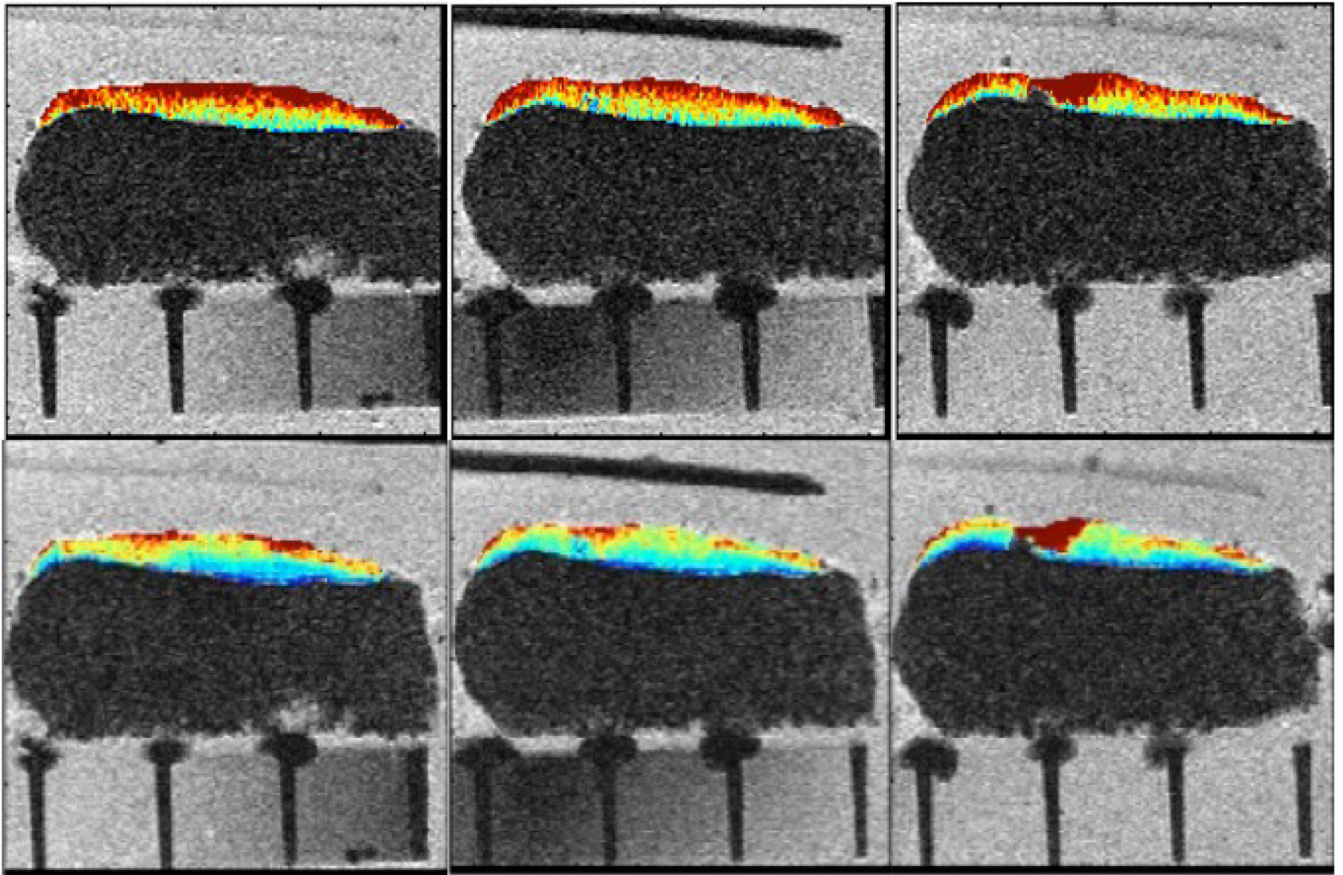


**Figure 5.** Three consecutive sections of ex vivo MRI with color-coded  $T_{1\rho}$  (top) and  $T_2$  (bottom) maps. The plastic tube indicates the center slice that was cut for histological analysis after ex vivo MRI.

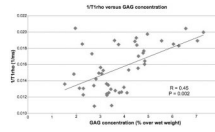


**Figure 6.** Significant correlation was found between  $R_{1\rho}$  ( $1/T_{1\rho}$ ) and GAG contents in human osteoarthritic cartilage.

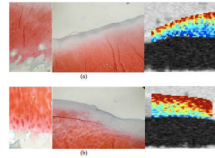


**Figure 7.**

Histology slides and  $T_{1\rho}$  maps from a lateral tibial plateau specimen. (a) The anterior section received a low overall Mankin score of 2, because of the presence of mild surface irregularities and the infiltration of blood vessel across the tidemark (left). The Safranin-O staining shows no detectable loss (center), corresponding to a score of 0. The adjacent biochemistry core in the anterior has a relatively high GAG concentration of 4.97%.  $T_{1\rho}$  agrees well with the histology and biochemistry findings, the region has a relatively low  $T_{1\rho}$  value of  $50.6 \pm 31.3$  ms (right); (b) The posterior section of the lateral tibial plateau received a higher overall Mankin score of 5, due to surface irregularities, pannus, cell cloning, and loss of safranin-O staining (left). The Safranin-O score was 1 due to focal loss of Safranin-O staining (center). The adjacent biochemistry core in the posterior has a relatively lower GAG concentration of 3.45%.  $T_{1\rho}$  agrees well with these findings, and the posterior region has a relatively high  $T_{1\rho}$  value of  $77.1 \pm 35.8$  ms (right).

**Table 1**

Mankin scoring system of cartilage degeneration.

	Grade		Grade
<b>I</b>	<b>Structure</b>	<b>III</b>	<b>Safranin-O Staining</b>
	Normal		Normal
	Surface irregularities		Slight reduction
	Pannus and surface irregularities		Moderate reduction
	Clefts to transitional zone		Severe reduction
	Clefts to radial zone		No dye noted
	Clefts to calcified zone		
Complete disorganization			
<b>II</b>	<b>Cells</b>	<b>IV</b>	<b>Tidemark Integrity</b>
	Normal		Intact
	Diffuse hypercellularity		Crossed by blood vessels
	Cloning		
	Hypocellularity		

**Table 2**

$T_{1\rho}$  and  $T_2$  measurement (in ms) at different orientation (degree relative to  $B_0$ ).

	90°	0°	54.7°
$T_{1\rho}$ (500Hz)	62.0 ± 5.9	59.4 ± 9.2	68.8 ± 4.7
$T_{1\rho}$ (1KHz)	72.7 ± 6.0	70.2 ± 5.9	77.7 ± 6.1
$T_2$	48.1 ± 11.8	47.3 ± 13.3	57.4 ± 11.6

**Table 3**

Biochemical measurements and relaxation times at the femoral condyle.

	Biochemistry		Relaxation times	
	GAG (%)	Collagen (%)	T <sub>1ρ</sub> (ms)	T2 (ms)
LIFC	4.5 ± 1.8	4.4 ± 1.8	62.4 ± 11.8	34.3 ± 8.6
LPFC	3.3 ± 0.7	6.9 ± 3.4	76.8 ± 7.9	52.8 ± 6.7
P	0.036	0.095	0.002	0.0002